Control of *Arabidopsis* meristem development by thioredoxin-dependent regulation of intercellular transport

Yoselin Benitez-Alfonso[a], Michelle Cilia[a,b,1], Adrianna San Roman[a,b], Carole Thomas[c], Andy Maule[c], Stephen Hearn[a], and David Jackson[a,2]

[a]Cold Spring Harbor Laboratory and [b]Watson School of Biological Sciences, Cold Spring Harbor Laboratory, Cold Spring Harbor, NY 11724; and [c]John Innes Centre, Norwich Research Park, Colney, Norwich NR4 7UH, United Kingdom

Cell-to-cell transport in plants occurs through cytoplasmic channels called "plasmodesmata" and is regulated by developmental and environmental factors. Callose deposition modulates plasmodesmal transport in vivo, but little is known about the mechanisms that regulate this process. Here we report a genetic approach to identify mutants affecting plasmodesmal transport. We isolated 5 mutants, named *gfp arrested trafficking* (*gat*), affected in GFP unloading from the phloem into the meristem. *gat1* mutants were seedling lethal and carried lesions in an *m*-type thioredoxin that is expressed in non-green plastids of meristems and organ primordia. Callose and hydrogen peroxide accumulated in *gat1* mutants, and WT plants subjected to oxidative conditions phenocopied the *gat1* trafficking defects. Ectopic expression of GAT1 in mature leaves increased plasmodesmal permeability and led to a delay in senescence and flowering time. We propose a role for the GAT1 thioredoxin in the redox regulation of callose deposition and symplastic permeability that is essential for meristem maintenance in *Arabidopsis*.

callose | cell-to-cell trafficking | plasmodesmata | redox regulation | thioredoxin m-type

Cell-to-cell communication is of fundamental importance during development and occurs in plants through specialized channels, named plasmodesmata (PD), which mediate the long- and short-distance transport of metabolites, proteins, and RNAs (1–4). Transport through PD can occur by either a non-targeted or a targeted pathway. Small and/or compact molecules, including metabolites and the GFP or the LEAFY transcription factor, are thought to diffuse through the channels in a non-targeted manner, but other proteins appear to interact with PD and move by a targeted mechanism (1–5). The size exclusion limit (SEL) is defined as the maximum size of molecules that can diffuse through PD, and the SEL varies in response to environmental and developmental conditions (1–3).

Intercellular trafficking can be controlled by modification of PD structure or occlusion by callose (6, 7). Callose synthesis is induced by developmental and stress signals (8, 9) and leads to constriction of PD during leaf senescence, abscission, or following biotic or abiotic stress (10, 11). Callose is degraded by beta-1,3-glucanases; plants deficient in these enzymes show a reduced PD SEL, whereas their overexpression promotes viral movement (12, 13). Although several studies highlight a correlation between levels of reactive oxygen species (ROS) and callose deposition (9, 10), little is known about the underlying molecular mechanisms or the significance of this process in PD regulation (11, 12).

To understand the regulation of PD trafficking, we performed a genetic screen assaying non-targeted PD transport of GFP. We isolated 6 mutants with loss of GFP movement and named them "*gfp arrested trafficking*" (*gat*, pronounced "gate"). Here we describe *gat1*, defective in the gene encoding thioredoxin m3. Thioredoxins function in the redox regulation of a broad spec-

trum of enzymes (14), and we provide evidence linking the loss of *GAT1* with the induction of callose and structural modification of PDs. We propose that GAT1 (TRX-m3) regulates symplastic trafficking that is crucial for meristem maintenance in *Arabidopsis*.

Results

Arabidopsis plants expressing GFP (15) from the phloem-specific *SUCROSE-H+SYMPORTER 2* gene promoter (p*SUC2*) passively transport GFP through PD from the phloem into surrounding tissues, including the root meristem (Fig. 1*A*) (16). These plants were mutagenized with ethyl methyl sulfonate (EMS), and we screened at 5–10 days after germination (dpg) for restriction in GFP movement in roots of about 1,000 M2 lines. Six mutants were identified that corresponded to 5 different loci.

Four of the mutants (*gat1, 2, 4*, and *5*) had a severe restriction of GFP transport out of the root phloem (Fig. 1*B* and Fig. S1). The GFP pattern in *gat1* and *2* was similar to that in plants expressing a non-mobile GFP (mGFP5-ER) from p*SUC2*. Indeed, in *gat1*, GFP transport out of the phloem companion cells (CC) was blocked (Fig. S2) (17). In contrast, in *gat4* and *gat5*, GFP moved into the provasculature approaching the meristem (Fig. S1). In *gat3*, GFP moved out of the phloem into the stele and the quiescent center (QC) but not into the endodermis (Fig. S1). Differences in GFP mobility also were reflected in the seedling phenotypes: although *gat1, 2, 4*, and *5* arrested at around 10 dpg with a short root and stunted or no true leaf primordial (Fig. 1), *gat3* seedlings did not show any obvious developmental defects (Fig. S1). We selected *gat1* for further characterization because our screen identified 2 potential alleles.

Because *gat1* seedlings arrested soon after germination, we wondered if embryo development was affected. Around one-fourth of the embryos from selfed heterozygous plants were delayed in development (Fig. 1 *E* and *F*, and Fig. S2). These smaller embryos were assumed to be *gat1*, because after germination we observed the same ratio of small seedlings defective in GFP transport. The mutant seedlings did not initiate obvious true leaf primordia. To investigate whether the shoot apical meristem (SAM) was formed properly, we used a reporter for *SHOOTMERISTEMLESS* (*STM*), a gene required for maintenance of the SAM (18). We found that *gat1* mutants either failed
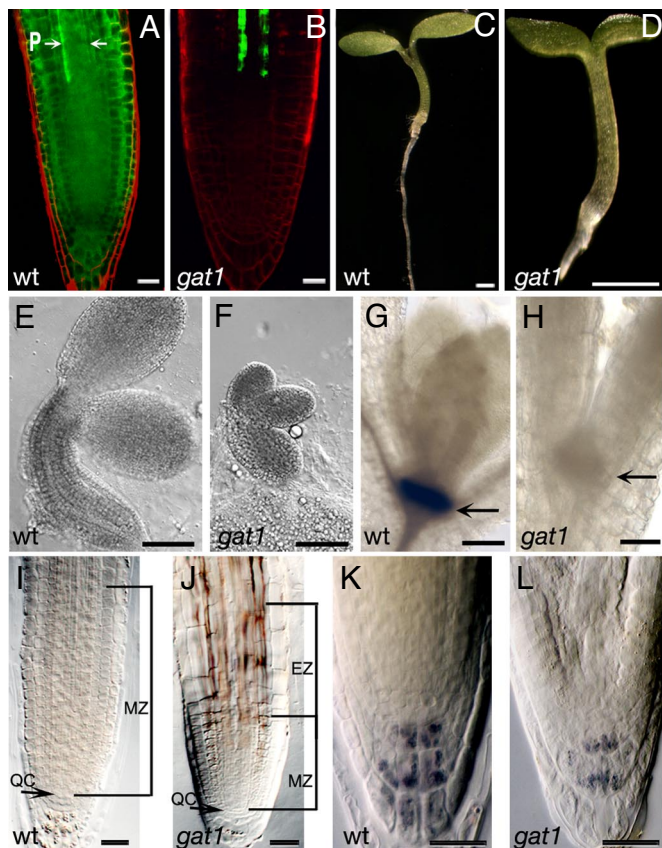
Fig. 1. GFP transport, embryo and seedling phenotypes of *gat1*. (*A*) WT seedlings expressing p*SUC2-GFP* show GFP diffusion out of the phloem (P, *arrows*) into the root meristem. (*B*) *gat1* mutants show severe restriction in GFP transport out of the phloem. Seedling phenotypes of (*C*) WT and (*D*) *gat1* mutants at 6 dpg show that *gat1* is smaller than WT. (*E*, *F*) Embryos at cotyledon stage show that *gat1* embryos also are smaller than WT. GUS staining of (*G*) WT and (*H*) *gat1* siblings shows that a p*STM-GUS* reporter is not expressed in the mutant (arrow indicates position of SAM). (*I*, *J*) The meristem zone (MZ) in *gat1* roots at 6 dpg is smaller than in WT. The elongation zone (EZ) also is indicated in *gat1* (*J*). Lugol's staining of (*K*) WT and (*L*) *gat1* collumela cells shows that fewer starch granules accumulated in the mutant. Scale bars represent 20 μm in *A*, *B*, and *I–L*, 1 mm in *C* and *D*, 100 μm in *E* and *F*, and 50 μm in *G* and *H*.

to express this reporter (31 of 40 mutants), or expression was very weak, suggesting that the SAM was not initiated or maintained (Fig. 1 *G* and *H*).

gat1 roots stopped growing at around 6 dpg, and the meristem zone (measured from the QC to the uppermost cells undergoing division, ref. 19) was smaller than in WT siblings ($n = 20$, $P < 0.0001$; Fig. 1 *I* and *J*). The elongation zone (the area of the root where cells elongate before differentiation) also was shorter in *gat1* than in WT roots, and fewer starch granules were observed in the columella cells (Fig. 1 *I–L*). This observation suggests that the arrested root growth might be caused by a lack of energy reserves, and we found that growth was partially rescued on media containing 1% sucrose (Fig. S2).

The defect in GFP transport in *gat1* mutants might be caused by an indirect effect on phloem development or in meristem identity. However, developmental reporters for the provasculature (JYB697, At2g18380) or QC (JYB1234, At5g17800) (Lee, Colinas, and Benfey, unpublished data) showed normal expression in *gat1*, suggesting that the phloem and QC were specified correctly (Fig. S2). We also observed normal expression of a translational GFP-fusion of ALTERED PHLOEM DEVELOPMENT (*APL*), a gene required for phloem identity (20), and a
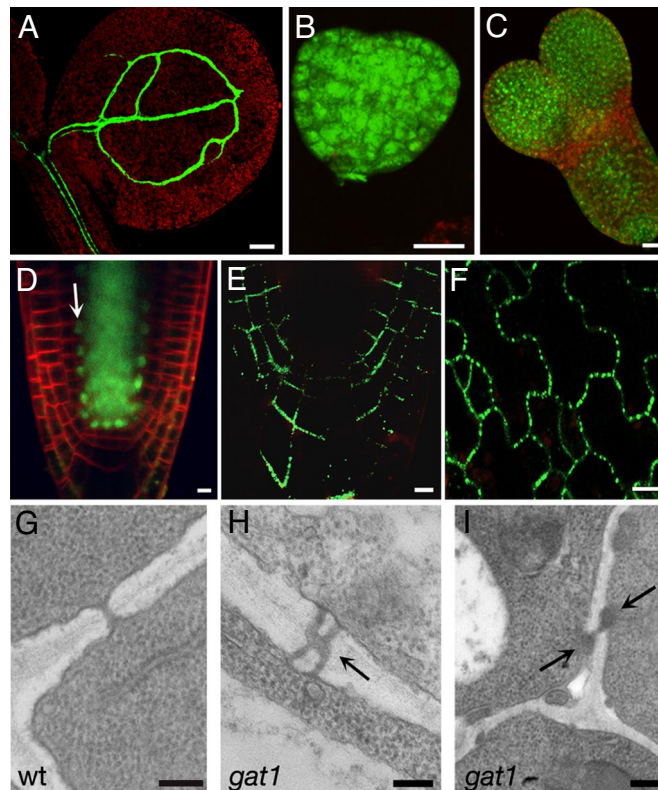

Fig. 2. *gat1* PD phenotypes. *gat1* seedlings expressing p*SUC2-GFP,* showing that GFP is restricted to the phloem in the shoot (*A*). Loading of HPTS in *gat1* heart (*B*) and torpedo (*C*) embryo stages indicates symplastic transport. (*D*) *gat1* seedlings expressing p*SHR-SHR-GFP* transport the fusion protein from the stele to the endodermis (*white arrow*). Expression of the fusion protein PDLP1A-YFP shows targeting to PDs in *gat1* root (*E*) and cotyledons (*F*). TEM analysis of root sections at 50 μm from the QC shows simple PD in WT (*G*) but branched (*H*) and occluded PD (*I*) in *gat1* (*arrows*). Scale bars represent 100 μm in *A*, 20 μm in *B–D* and *F*, 5 μm in *E*, and 0.2 μm in *G–I*.

reporter for *PLETHORA1*, a gene essential for QC specification (Fig. S2) (21). However, the smaller meristem and lack of growth in *gat1* indicates a failure to maintain root meristem function after germination.

Further imaging of *gat1* seedlings showed that GFP movement was restricted not only in the root meristem but also in shoot tissues, suggesting a general PD defect (Fig. 2*A*). We next asked if *gat1* mutants formed functional PDs. WT embryos traffic the small (0.5 kDa) tracer dye 8-hydroxypyrene-1,3,6-trisulfonic acid, but larger dyes become restricted as the embryos develop (22). No differences were observed in dye movement between *gat1* and WT embryos (Fig. 2 *B* and *C*). Therefore the symplastic connectivity defects in *gat1* either form late in embryogenesis or might be restricted to the phloem, which is not assayed in the dye-loading studies. Alternatively, they might result from a down-regulation of PD SEL that does not affect the diffusion of this small dye. We also asked if proteins that traffic by a targeted mechanism are able to move in *gat1* mutants. We assayed the movement of SHORT-ROOT (SHR), a 59-kDa protein that belongs to the GRAS family of transcription factors and is required for specification of the ground tissue. SHR traffics in a presumed PD-targeted manner from the stele to the endodermis (23). Imaging of *gat1* seedlings expressing p*SHR-SHR-GFP* showed that transport of SHR was not affected (Fig. 2*D*). Next, to investigate whether PDs were present in *gat1*, we used a YFP fusion of PLASMODESMATA-LOCATED PROTEIN 1 (PDLP1A) (24). In *gat1*, we found punctate labeling in the cell
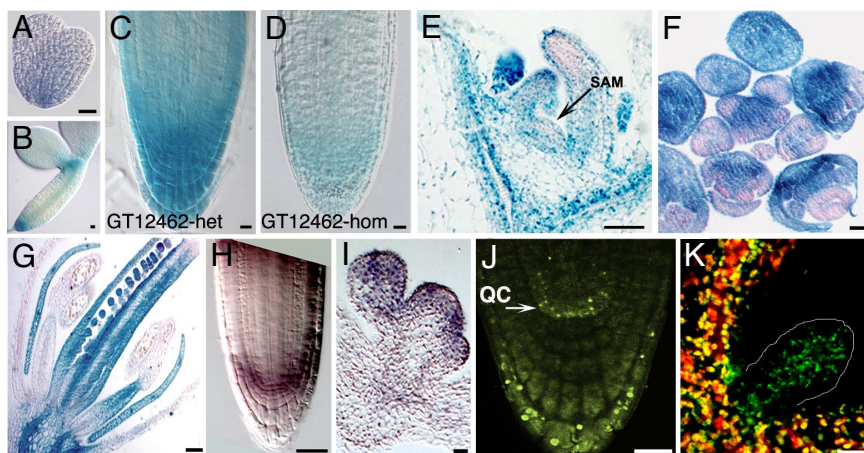
Fig. 3. GAT1 is expressed in meristems and primordia and localizes to plastids. GUS staining of the gene trap line *gat1–3* shows expression in embryos from heart (*A*) and cotyledon (*B*) stages, in root meristem (*C*, *D*), vegetative apex including SAM vasculature (*arrow*) (*E*), inflorescences (*F*), and flowers (*G*). The homozygous gene trap insertion shows reduced expression (*D*) compared with heterozygote (*C*). In situ hybridization confirms *GAT1* expression in root (*H*) and floral meristems (*I*). (*J*) Plants expressing GAT1:YFP under the endogenous promoter show native expression in non-green plastids of QC (*arrows*) and columella cells. (*K*) Confocal images of seedling shoots from plants overexpressing GAT1:YFP show green fluorescence in both photosynthetic and non-photosynthetic tissues (*marked*) that co-localizes with chlorophyll red autofluorescence. Scale bars represent 10 μm in *A*, *B*, and *E* and 20 μm in *C*, *D*, and *F*–*K*.

walls, suggesting that PD targeting was unaltered (Fig. 2 *E* and *F*). We next used transmission electron microscopy (TEM) to investigate whether PD ultrastructure was compromised. Root sections were taken at ≈ 50 μm above the QC, which corresponds to the meristem zone. WT and *gat1* showed a similar organization of dividing cells in this region (not shown). PD frequency was similar in mutants and WT (WT $= 0.41 \pm 0.11$ PD/μm of cell wall; *gat1* $= 0.49 \pm 0.04$ PD/μm of cell wall), but altered PDs were observed in the mutant (Fig. 2 *G–I*). PDs in WT were unbranched, as expected, but in *gat1* $\approx 9\%$ of the PD were branched, and $\approx 5\%$ appeared to be occluded (in total, 20 of 155 PDs were affected) (Fig. 2 *G–I*). In summary, *gat1* roots formed PD at a normal frequency, but their structure was modified, presumably causing the restricted GFP trafficking phenotype.

We mapped *gat1* to a region containing 6 predicted genes, and complementation tests with insertional mutants in those genes indicated that *GAT1* encodes the predicted thioredoxin m3 (*TRX-m3*; At2g15570). To confirm this result, heterozygous *gat1* plants were transformed with the WT gene, and complementation was checked by segregation analysis in T2 lines. The progeny of 18 of 38 individual T1 plants showed the expected 1/16 segregation for complementation. We identified 5 additional *gat1* alleles, *emb57*:*gat1–2* (http://mutant.lse.okstate.edu); GT12462:*gat1–3*; ET11294:*gat1–4*; ET3878:*gat1–5* (http://genetrap.cshl.org); and SALK_061968:*gat1–6* (http://signal.salk.edu) (Fig. S3). We introduced the p*SUC2-GFP* reporter into *gat1–3* and found restricted GFP movement and developmental phenotypes identical to *gat1–1* (not shown). *gat1-3* contains a *Dissociation* transposon insertion in the intron, which affects gene expression (Fig. 3*D*). The GAT1–β-glucuronidase (GUS) fusion protein made by this allele is predicted to be inactive, because the insertion, upstream of the thioredoxin domain, alters splicing and creates an aberrant protein. Interestingly, the original allele, *gat1–1*, lacked any sequence changes. Molecular analysis suggested that this allele probably is an epiallele, because it showed hypermethylation and could be partially complemented by crossing to *ddm1* mutants (Fig. S3).

GAT1:TRX-m3 encodes a protein with a predicted *N*-terminal chloroplast-targeting signal followed by a thioredoxin domain (Fig. S3). Using the GUS reporter in the *gat1–3* gene trap line, we observed expression during embryogenesis at the transition from heart to torpedo stage that was strongest in the root meristem (Fig. 3*A*). At the cotyledon stage, expression was in root and shoot meristems, with weak staining in provascular tissues (Fig. 3*B*). Expression persisted in the seedling root meristem, shoot apex, and vasculature (Fig. 3 *C* and *E*), and was reduced when the gene trap insertion was homozygous (Fig. 3*D*). Strong GUS expression was maintained in inflorescence and floral meristems (Fig. 3*F*) and in petal, stamen, and carpel primordia (Fig. 3*G*). Similar expression was detected by in situ hybridization of roots and floral meristems (Fig. 3 *H* and *I*).

Previous studies suggested that GAT1:TRX-m3 localizes to plastids (25). We fused YFP at the *C* terminus of the protein and found by transient expression that TRX-m3 localized to presumed proplastids (Fig. S3). Plants expressing p*GAT1-GAT1-YFP* showed localization to organelles resembling immature plastids in the root meristem and columella (Fig. 3*J*) and vasculature (not shown). Co-localization of YFP expression with chlorophyll autofluorescence in p*35S-GAT1-YFP* transgenic plants indicated that the overexpressed protein co-localized with chloroplasts (Fig. 3*K* and Fig. S3).

Because thioredoxins function in redox homeostasis and regulate the activity of thiol-containing enzymes (14), we hypothesized that the redox state might be altered in *gat1* mutants. Staining of H_2O_2 with 3,3′-diaminobenzidine (DAB) showed hyperaccumulation of ROS in *gat1* root meristems (Fig. 4 *A* and *B*). This difference was quantified by the eFOX method, and a significant increase in hydrogen peroxide content was detected in the mutant seedlings (Table S1). Callose synthesis is induced by oxidative conditions (9), and we found that callose levels were approximately doubled in *gat1* (Fig. 4 *I* and *J*, and Fig. S4).

To test if ROS-mediated callose deposition was sufficient to explain the loss of GFP transport in *gat1*, we germinated WT seedlings expressing *pSUC2-GFP* on media supplemented with alloxan (1.5 mM) or paraquat (1 μM), which induce the production of H_2O_2, or O_2^-, respectively (26, 27). As expected, high concentrations of H_2O_2 were detected in seedlings germinated on these oxidants (Fig. 4 *C* and *D*), and we found an arrest in root growth (not shown) and in GFP transport resembling that in *gat1* mutants (Fig. 4 *G* and *H*). In addition, callose accumulation was increased in oxidant-treated seedlings (Fig. 4 *K* and *L*, and Fig. S4). Together, these results show that treatment of WT plants with oxidants had an effect similar to the loss of *GAT1:TRX-m3*, suggesting a role for GAT1 in redox homeostasis.

GAT1 is expressed in meristems, where it regulates redox state and PD permeability. To investigate whether GAT1 expression
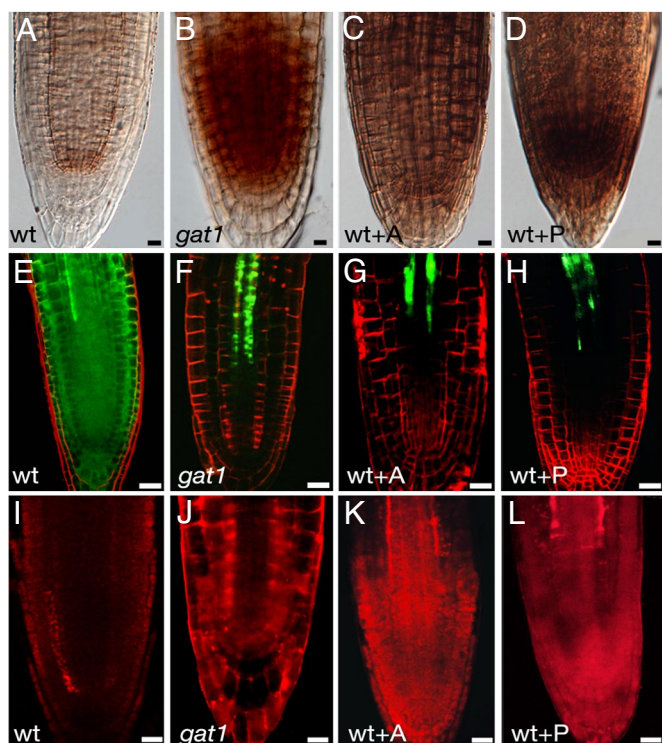
Fig. 4. WT seedlings germinated in oxidants phenocopy *gat1*. DAB staining of (*A*) WT, (*B*) *gat1*, and WT seedlings treated with (*C*) alloxan (WT+A) or (*D*) paraquat (WT+P). *gat1* and oxidant-treated seedlings accumulated ROS in the root meristem. WT seedlings expressing p*SUC2-GFP* and treated with (*G*) alloxan (WT+A) or (*H*) paraquat (WT+P) show defects in GFP diffusion and callose deposition (aniline blue staining shown in red, *K*, *L*) similar to those in *gat1* mutants (*F*, *J*). Nontreated WT seedlings are shown in *E* and *I*. Scale bars represent 20 μm.

Fig. 5. Ectopic expression of GAT1 promotes trafficking and delays senescence and flowering time. (*A*) The percentage of target sites in WT or p*SAG12-GAT1* leaves that transported (> 2 cells) or did not transport (1 cell) GFP after bombardment with p*35S-GFP*. A higher percentage of events show GFP diffusion in p*SAG12-GAT1*. Dark-induced senescence of detached leaves from (*B*) WT and (*C*) p*SAG12-GAT1* plants at 5 days after induction show that p*SAG12-GAT1* leaves were delayed in senescence. p*SAG12-GAT1* plants also were delayed in flowering in short-day conditions (*D*). Plants are 12 weeks old. The WT plant flowered 3 weeks earlier.

is sufficient to control PD permeability in tissues where it is not normally expressed, we ectopically expressed GAT1 using the *SENESCENCE-ASSOCIATED GENE 12* promoter (p*SAG12*) (28). *SAG12* encodes a cysteine protease expressed in fully expanded leaves, before senescence (28). We measured GFP diffusion in mature leaves of p*SAG12-GAT1* plants by biolistic experiments. More cells showed GFP diffusion in p*SAG12-GAT1* leaves than in WT leaves, indicating that non-targeted PD trafficking was significantly enhanced (> 150 bombardment sites from 3 independent tests, $P < 0.0001$; Fig. 5*A*).

The p*SAG12-GAT1* plants also showed a delay in flowering time and in senescence (Fig. 5). Senescence was assayed by dark-induced loss of chlorophyll in detached leaves (Fig. 5 *B* and *C*). p*SAG12-GAT1* plants retained more chlorophyll after induction (Table S1). Flowering time was measured by counting the number of leaves at the time the first flower bud was visible (29) and the number of days from sowing to the appearance of the first flower bud. In our long-day conditions, WT plants flowered at around 17–20 dpg with 8–12 leaves, whereas p*SAG12-GAT1* plants flowered at 30 ± 7 dpg with 28 ± 10 leaves ($n = 20$, $P < 0.001$), indicating that GAT1 ectopic expression delayed flowering. This delay in flowering also was evident in short-day conditions (Fig. 5*D*).

In summary, we used a screen to identify mutants that are impaired in cell-to-cell trafficking of GFP. We identified *gat1* as the putative thioredoxin-m3. GAT1:TRX-m3 regulates redox homeostasis and callose accumulation. We found that GAT1:TRX-m3 is necessary to maintain symplastic permeability in the meristem and that its ectopic expression is sufficient to enhance PD transport in mature tissues and affects senescence
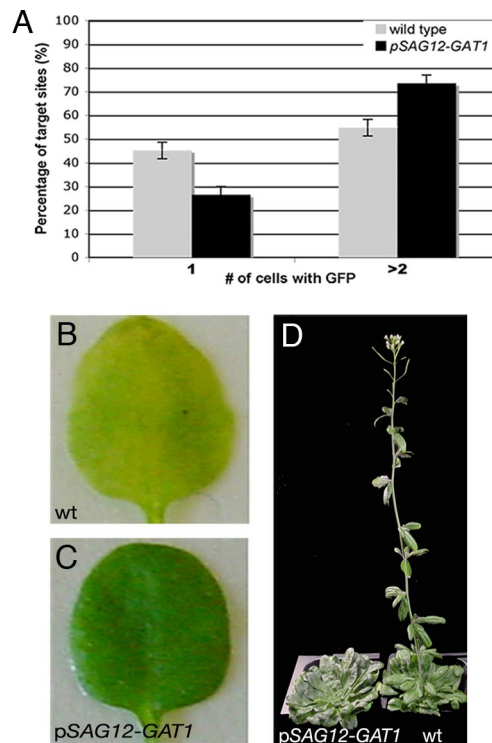
and flowering time. These data suggest that GAT1:TRX-m3 is an important regulator of PD cell-to-cell communication and meristem maintenance in vivo.

Discussion

Because of the difficulty in purifying PD from cell walls (30) and the likelihood that PD mutants will be lethal (22), our understanding of the molecular structure and mechanisms regulating PD permeability is relatively poor. Here we used a genetic screen to identify factors that regulate PD SEL. Our screen was complementary to one for increased SEL mutants (*ise*), which showed enhanced PD transport of a symplastic dye during embryogenesis (22, 31) and also found mutants defective in embryo development. Most of the mutants isolated in our screen were recessive and GFP transport out of the phloem was blocked. The lethality of these mutations was not surprising, because the phloem transports essential metabolites, proteins, and hormones from photosynthetic source tissues to actively growing sink tissues, including meristems (32). The high transport capacity of sink organs declines as their tissues mature and is correlated with a switch from simple to branched PDs (7, 33). Therefore we proposed that *gat* mutants fail to maintain a high symplastic transport capability, associated with high PD SEL, in meristems and other sink tissues, presumably leading to their growth arrest and lethality.

The expression of developmental markers for phloem, QC, and ground tissues was unaffected in *gat1* mutants. This result suggests that the loss of trafficking was not caused by abnormal phloem differentiation or tissue identity but instead was caused

Benitez-Alfonso *et al.*

by specific plasmodesmal defects. Although PDs were present and functional in *gat1*, TEM analysis revealed that some PDs were modified. PD branching is correlated with reduced SEL (7, 33), and occlusion caused by callose deposition also can inhibit transport (11). *gat1* mutants accumulated high levels of callose, particularly in the root meristem, where trafficking of GFP was severely affected. Together these results suggest that structural modification (from simple to branched) and/or occlusion of PD by callose was responsible for the blocking of symplastic GFP transport in *gat1*.

GAT1 encodes the plastidial thioredoxin *TRX-m3*, which belongs to a family of 4 predicted plastidial TRXs that are thought to function in maintenance of redox homeostasis (14). In contrast to other *m*-type thioredoxins, TRX-m3 does not have in vitro affinity to or activity for standard substrates, and it failed to complement a yeast *trx*-null mutant or to confer tolerance to oxidative stresses; therefore its function has been a mystery (25, 34). Our finding that *gat1* mutants accumulate ROS supports the hypothesis that this gene does function in redox homeostasis, but, unlike other family members, its expression was limited to plastids in non-green tissues, such as meristems, vasculature, and developing sink tissues.

The accumulation of ROS in *gat1* mutants probably is responsible for callose accumulation, as described in other instances (9, 35). Therefore, although GAT1:TRX-m3 does not target to PD specifically, its effect on cellular redox status seems to play a role in the regulation of PD permeability. In support of this idea, we found that *gat1* trafficking defects were phenocopied in WT plants treated with chemical oxidants. As in *gat1*, increased callose deposition was found in the root meristem of oxidant-treated plants. Further evidence for redox regulation of PD SEL comes from studies of the maize mutant *sucrose export defective 1* (*sxd1*) and its *Arabidopsis* homologs *vte1* and *vte2*. These mutants also produce more callose and aberrant PD structures that correlate with a reduced sucrose export from source leaves (35, 36). The mechanism by which these genes regulate PD trafficking is unknown, although *vte1* and *vte2* encode enzymes essential in the synthesis of vitamin E, which protects against photo-oxidative stress (35). Therefore GAT1:TRX-m3 and SXD1/VTE may have analogous roles in redox regulation of symplastic transport, with GAT1:TRX-m3 functioning in meristems and immature tissues, and SXD1/VTE functioning in mature organs.

Ectopic expression of GAT1 using the *SAG12* promoter enhanced PD transport in mature tissues, measured by quantification of GFP diffusion. This result indicates that GAT1 not only was necessary but also was sufficient to regulate PD permeability. During development, tissue maturation is correlated with a reduction in PD SEL, and development terminates in senescence that is associated with mobilization and phloem export of nutrients (10). The transition to flowering also is correlated with dynamic changes in PD permeability (37). Interestingly, the p*SAG12-GAT1* transgenic plants showed a delay in both senescence and in flowering time. We hypothesize that these phenotypes result from alterations in PD SEL that are caused by ectopic GAT1 expression. In summary GAT1:TRX-m3 seems to play a crucial function in maintenance of a high capacity for symplastic transport, characteristic of meristems and immature tissues. This function might be executed indirectly by a general reductive effect, because callose levels are under redox control (35). Alternatively, the effect might be more direct through activation of an early step in callose synthesis in plastids. The impact of altered redox homeostasis in plant development also has been described in other circumstances. For example, cell proliferation and root hair growth depend on redox status (38), and flower development requires 2 glutaredoxins involved in oxidative stress responses (39). Recent studies have found that amylo-

plasts and other non-photosynthetic plastids also contain a ferredoxin-linked TRX system (40, 41); therefore this system also might contribute to the redox regulation of symplastic trafficking and meristem development. Our results support a growing body of evidence that regulation of PD permeability is critical in coordinating whole-plant growth and development and could be used to modulate plant growth in response to environmental or endogenous signals.

Materials and Methods

Molecular Biology. Cytoplasmic mGFP6 (GFP) was amplified from the vector pmGFP6 (a gift from J. Haseloff, Cambridge, UK) and replaced *mGFP5-ER* in the p35S-*mGFP5-ER* binary vector (15) using the restriction sites BglII and HindIII. The p*SUC2-GFP* and p*SUC2-mGFP5-ER* constructs were made by replacing the *35S* promoter with the *SUC2* promoter (PCR amplified from Col genomic DNA with primers cited in Table S2).

Gateway technology (Invitrogen) was used to generate the other clones. The *GAT1:TRX-m3* gene was amplified from genomic DNA and subcloned into pDONR207 (AttB-*GAT1*) (Table S2). YFP was fused as described (42). (Primers are listed in Table S2). *SAG12* and *GAT1* promoters were amplified and cloned in the binary vector pAM-PAT GW (primers are listed in Table S2) (43), and the final constructs were obtained by LR reaction.

Standard protocols were used for *Arabidopsis* DNA and RNA isolation (44). Mapping by bulk segregation analysis was carried out as described (45), followed by fine mapping using markers from TAIR and Cereon databases (http://www.arabidopsis.org).

Plant Work and Histology. Plants were grown under fluorescent lights in a growth chamber or greenhouse with short-day conditions (8 h of light at 22 °C, ≈70% relative humidity) or long-day conditions (22 °C, 16 h of light, ≈70% relative humidity) as described (46). Seeds were germinated on Murashige and Skoog (MS) plates (44), and when indicated the medium was supplemented with 1% sucrose, 1.5 mM alloxan, or 1 μM paraquat (Sigma-Aldrich).

Transgenic *Arabidopsis* was obtained by *Agrobacterium*-mediated floral dip (44). For mutagenesis, a p*SUC2-GFP* homozygous single-insertion line was selected. Approximately 2,000 seeds were soaked in 17 mM of EMS (Sigma-Aldrich) for 12 h with gentle rocking at room temperature. M1 seeds were washed and planted, and M2 seedlings were screened using a Zeiss Axioplan microscope.

Imaging was performed using a Zeiss LSM510 confocal microscope. GFP was excited at 488 nm, and emitted light was captured at 505–550 nm. Chlorophyll autofluorescence and counterstaining with FM4–64 or propidium iodide was detected using a 585-nm long-pass filter. Callose was stained with 0.005% aniline blue solution in sodium phosphate buffer, pH 9, and was imaged using an excitation of 405 nm and emission at 460 nm or at 585 nm. Dye loading, GUS, staining and in situ hybridization experiments were performed as described (22, 44, 47). A portion of the 3′ UTR and the last exon was used as a probe (amplified with the primers *GAT1*-3′ utr, Table S2). H_2O_2 was stained by vacuum infiltration with 0.1 mg/ml DAB in 50 mM Tris buffer, pH 5. Seedlings were dipped in Lugol's solution (2% KI and 1% I_2 in HCl 0.2N) for 2 min to stain starch granules. These samples were mounted in Hoyer's solution (48) and visualized using differential interference contrast microscopy (Leica DMRB microscope). Hoyer's solution also was used to clear seeds and roots for microscopy.

For TEM, we used a protocol previously described (49), except that fixation was in 2% paraformaldehyde, 2% glutaraldehyde, 0.1% (wt/vol) tannic acid, 50 mM sodium cacodylate buffer, pH 6.8, for 24 h at 4 °C. The sections were examined with an Hitachi 7000 transmission electron microscope.

For biolistic transformation, we followed published protocols (50). Statistical non-parametric Mann-Whitney analysis was performed using GraphPad Prism software (GraphPad Software).

Senescence was assayed using the fourth fully expanded leaf of ≈20-day-old plants placed in MS solution and kept in the dark. Senescence was estimated by loss in chlorophyll pigments 5 and 15 days after the induction.

PLANT BIOLOGY

1. Benitez-Alfonso Y, Cantrill L, Jackson D (2006) in *Cell-Cell Channels*, eds. Baluska F, Volkmann D, Barlow PW (Landes Bioscience, Austin, TX).
2. Crawford KM, Zambryski PC (2001) Non-targeted and targeted protein movement through plasmodesmata in leaves in different developmental and physiological states. *Plant Physiol* 125:1802–1812.
3. Lucas WJ, Lee JY (2004) Plasmodesmata as a supracellular control network in plants. *Nat Rev Mol Cell Biol* 5:712–726.
4. Cilia M, Jackson D (2004) Plasmodesmata form and function. *Curr Opin Cell Biol* 16:500–506.
5. Kurata T, Okada K, Wada T (2005) Intercellular movement of transcription factors. *Curr Opin Plant Biol* 8:600–605.
6. Kim JY (2005) Regulation of short-distance transport of RNA and protein. *Curr Opin Plant Biol* 8:45–52.
7. Oparka KJ, et al. (1999) Simple, but not branched, plasmodesmata allow the nonspecific trafficking of proteins in developing tobacco leaves. *Cell* 97:743–754.
8. Rinne PLH, van der Schoot C (2003) Plasmodesmata at the crossroads between development, dormancy, and defense. *Can J Bot* 81:1182–1197.
9. Sivaguru M, et al. (2000) Aluminum-induced 1−>3-beta-D-glucan inhibits cell-to-cell trafficking of molecules through plasmodesmata. A new mechanism of aluminum toxicity in plants. *Plant Physiol* 124:991–1006.
10. Jongebloed U, et al. (2004) Sequence of morphological and physiological events during natural ageing and senescence of a castor bean leaf: Sieve tube occlusion and carbohydrate back-up precede chlorophyll degradation. *Physiol Plant* 120:338–346.
11. Radford JE, Vesk M, Overall RL (1998) Callose deposition at plasmodesmata. *Protoplasma* 201:30–37.
12. Iglesias VA, Meins F, Jr., (2000) Movement of plant viruses is delayed in a beta-1,3-glucanase-deficient mutant showing a reduced plasmodesmatal size exclusion limit and enhanced callose deposition. *Plant J* 21:157–166.
13. Levy A, Erlanger M, Rosenthal M, Epel BL (2007) A plasmodesmata-associated beta-1,3-glucanase in *Arabidopsis*. *Plant J* 49:669–682.
14. Vieira Dos Santos C, Rey P (2006) Plant thioredoxins are key actors in the oxidative stress response. *Trends Plants Sci* 11:329–334.
15. Haseloff J, Siemering KR, Prasher DC, Hodge S (1997) Removal of a cryptic intron and subcellular localization of green fluorescent protein are required to mark transgenic *Arabidopsis* plants brightly. *Proc Natl Acad Sci USA* 94:2122–2127.
16. Imlau A, Truernit E, Sauer N (1999) Cell-to-cell and long-distance trafficking of the green fluorescent protein in the phloem and symplastic unloading of the protein into sink tissues. *Plant Cell* 11:309–322.
17. Stadler R, et al. (2005) Expression of GFP-fusions in *Arabidopsis* companion cells reveals non-specific protein trafficking into sieve elements and identifies a novel post-phloem domain in roots. *Plant J* 41:319–331.
18. Kirch T, Simon R, Grunewald M, Werr W (2003) The DORNROSCHEN/ENHANCER OF SHOOT REGENERATION1 gene of *Arabidopsis* acts in the control of meristem cell fate and lateral organ development. *Plant Cell* 15:694–705.
19. Maloof JN (2004) Plant development: Slowing root growth naturally. *Curr Biol* 14:R395–396.
20. Bonke M, et al. (2003) APL regulates vascular tissue identity in *Arabidopsis. Nature* 426:181–186.
21. Aida M, et al. (2004) The PLETHORA genes mediate patterning of the *Arabidopsis* root stem cell niche. *Cell* 119:109–120.
22. Kim I, et al. (2002) Identification of a developmental transition in plasmodesmatal function during embryogenesis in *Arabidopsis thaliana. Development* (Cambridge, UK) 129:1261–1272.
23. Nakajima K, Sena G, Nawy T, Benfey PN (2001) Intercellular movement of the putative transcription factor SHR in root patterning. *Nature* 413:307–311.
24. Thomas CL, et al. (2008) Specific targeting of a plasmodesmal protein affecting cell-to-cell communication. *PLoS Biol* 6:e7.
25. Collin V, et al. (2003) The *Arabidopsis* plastidial thioredoxins: New functions and new insights into specificity. *J Biol Chem* 278:23747–23752.
26. Sweetlove LJ, et al. (2002) The impact of oxidative stress on *Arabidopsis* mitochondria. *Plant J* 32:891–904.
27. Pasternak T, Potters G, Caubergs R, Jansen MA (2005) Complementary interactions between oxidative stress and auxins control plant growth responses at plant, organ, and cellular level. *J Exp Bot* 56:1991–2001.
28. Noh YS, Amasino RM (1999) Identification of a promoter region responsible for the senescence-specific expression of SAG12. *Plant Mol Biol* 41:181–194.
29. Putterill J, et al. (1995) The CONSTANS gene of *Arabidopsis* promotes flowering and encodes a protein showing similarities to zinc finger transcription factors. *Cell* 80:847–857.
30. Bayer E, Thomas CL, Maule AJ (2004) Plasmodesmata in *Arabidopsis thaliana* suspension cells. *Protoplasma* 223:93–102.
31. Kobayashi K, et al. (2007) INCREASED SIZE EXCLUSION LIMIT 2 encodes a putative DEVH box RNA helicase involved in plasmodesmata function during *Arabidopsis* embryogenesis. *Plant Cell* 19:1885–1897.
32. Oparka KJ, Cruz SS (2000) The great escape: Phloem transport and unloading of macromolecules. *Annu Rev Plant Physiol Plant Mol Biol* 51:323–347.
33. Roberts IM, et al. (2001) Dynamic changes in the frequency and architecture of plasmodesmata during the sink-source transition in tobacco leaves. *Protoplasma* 218:31–44.
34. Issakidis-Bourguet E, Mouaheb N, Meyer Y, Miginiac-Maslow M (2001) Heterologous complementation of yeast reveals a new putative function for chloroplast m-type thioredoxin. *Plant J* 25:127–135.
35. Maeda H, Song W, Sage TL, DellaPenna D (2006) Tocopherols play a crucial role in low-temperature adaptation and phloem loading in *Arabidopsis. Plant Cell* 18:2710–2732.
36. Russin WA, et al. (1996) Modification of a specific class of plasmodesmata and loss of sucrose export ability in the sucrose export defective1 maize mutant. *Plant Cell* 8:645–658.
37. Gisel A, Hempel FD, Barella S, Zambryski P (2002) Leaf-to-shoot apex movement of symplastic tracer is restricted coincident with flowering in *Arabidopsis. Proc Natl Acad Sci USA* 99:1713–1717.
38. Sanchez-Fernandez R, et al. (1997) Cell proliferation and hair tip growth in the *Arabidopsis* root are under mechanistically different forms of redox control. *Proc Natl Acad Sci USA* 94:2745–2750.
39. Xing S, Rosso MG, Zachgo S (2005) ROXY1, a member of the plant glutaredoxin family, is required for petal development in *Arabidopsis thaliana. Development* 132:1555–1565.
40. de Dios Barajas-Lopez J, et al. (2007) Localization in roots and flowers of pea chloroplastic thioredoxin f and thioredoxin m proteins reveals new roles in nonphotosynthetic organs. *Plant Physiol* 145:946–960.
41. Balmer Y, et al. (2006) A complete ferredoxin/thioredoxin system regulates fundamental processes in amyloplasts. *Proc Natl Acad Sci USA* 103:2988–2993.
42. Tian GW, et al. (2004) High-throughput fluorescent tagging of full-length *Arabidopsis* gene products in plants. *Plant Physiol* 135:25–38.
43. Weinl C, et al. (2005) Novel functions of plant cyclin-dependent kinase inhibitors, ICK1/KRP1, can act non-cell-autonomously and inhibit entry into mitosis. *Plant Cell* 17:1704–1722.
44. Weigel D, Glazebrook J (2002) *Arabidopsis, a Laboratory Manual* (CSHL Press, Cold Spring Harbor, NY).
45. Lukowitz W, Gillmor CS, Scheible WR (2000) Positional cloning in *Arabidopsis*. Why it feels good to have a genome initiative working for you. *Plant Physiol* 123:795–805.
46. Kim JY, Yuan Z, Jackson D (2003) Developmental regulation and significance of KNOX protein trafficking in *Arabidopsis. Development* 130:4351–4362.
47. Rosen B, Beddington RS (1993) Whole-mount in situ hybridization in the mouse embryo: gene expression in three dimensions. *Trends Genet* 9:162–167.
48. Liu CM, Meinke DW (1998) The titan mutants of *Arabidopsis* are disrupted in mitosis and cell cycle control during seed development. *Plant J* 16:21–31.
49. Haritatos E, Medville R, Turgeon R (2000) Minor vein structure and sugar transport in *Arabidopsis thaliana. Planta* 211:105–111.
50. Kim JY, et al. (2002) Intercellular trafficking of a KNOTTED1 green fluorescent protein fusion in the leaf and shoot meristem of *Arabidopsis. Proc Natl Acad Sci USA* 99:4103–4108.

Benitez-Alfonso *et al.*